CALCULATION OF FLOWS WITH SEPARATION, HEAT TRANSFER, AND SWIRL BY MEANS OF BOUNDARY-LAYER EQUATIONS

V. I. Vasil'ev and S. V. Khokhlov

UDC 532.526.2

It has been shown [1] that flows with thin closed separation zones can be calculated by means of boundary-layer equations if the inverse problem for these equations is considered and if interaction with the external inviscid flow is taken into account. This approach is called the direct–inverse method and is commonly used to describe flows around profiles [2]. We have previously [3, 4] developed a computational procedure that can be used to calculate laminar and turbulent separation flows in an interior section of a wide channel [3] and in a channel with a separator [4].

In the present article we use the direct–inverse method to analyze flows with heat transfer and swirl. Whereas the relationship between the dynamical and thermal characteristics have been well studied for nonseparation flows [5], it has not received adequate attention in the case of flows with separation. In particular, the increase in the heat fluxes in the vicinity of the reattachment point needs to be investigated in greater detail; the direct–inverse method should be useful in this regard. Here we consider laminar separation flow with heat transfer and show that the results of the calculations exhibit satisfactory agreement with the results of numerical solution of the Navier–Stokes equations and with experimental data [6].

In boundary-layer calculations for swirled flow the pressure across the layer is usually assumed to be constant, and nonseparation flow regimes are investigated [7]. In the present article we investigate swirled flows with separation on the assumption that the transverse pressure gradient in the boundary layer is equalized by centrifugal forces. Boundary-layer separation on a cylindrical surface is possible under these conditions. We also investigate self-similar solutions of the boundary-layer equations with swirl, specifically the self-similar solutions corresponding to flow with reverse currents.

1. We investigate two types of laminar flows of an incompressible fluid: planar flow over a surface whose contour is described in Cartesian coordinates x, y by the equation $y = r(x)$ and whose temperature differs from the freestream temperature, but with a temperature factor close to unity, so that the fluid can be regarded as incompressible with a constant transport coefficient (Fig. 1a); axisymmetrical swirled flow in a channel whose wall contours are described in cylindrical coordinates x, y by the equations $y = r_{\pm}(x)$, the plus sign corresponding to the upper wall, and the minus sign to the lower wall (Fig. 1b). The longitudinal scale of nonuniformity on the free surface or the length of the transition zone of the channel (L) is adopted as the characteristic length, and the freestream velocity or the duct entry velocity (U_∞) is taken as the characteristic velocity. The Reynolds number $Re = U_\infty L/\nu$ (ν is the kinematic viscosity) is assumed to be large, and the transverse scale of nonuniformity of the surfaces are considered to be of the order of the boundary-layer thickness δ [$\Delta_y r = O(\delta)$], so that the separation zones are thin.

The flow is partitioned into viscous and inviscid regions, between which strong interaction is possible; the separation zone is located within the viscous region. In the case of channel flow we assume that the characteristic length of the inviscid core is of the same order as the width of the channel, and $\delta_{\pm} \ll r_+ - r_-$; in addition, we assume that $r_{\pm} \gtrsim L$. The flow in the viscous region is described by boundary-layer equations, for which (to avoid a singularity at the separation point) the inverse problem is solved, i.e., the displacement thickness is given, and the longitudinal pressure gradient is determined. The flow in the inviscid region is described by the Euler equations, which are solved in the linear approximation for the stated problems. The necessary displacement thickness is determined from the condition for matching the solutions in the viscous and inviscid flow regions.

Moscow. Translated from Prikladnaya Mekhanika i Tekhnicheskaya Fizika, No. 2, pp. 36-43, March-Aril, 1993. Original article submitted July 23, 1991; revision submitted March 27, 1992.

 0021-8944/93/3402-0184$12.50

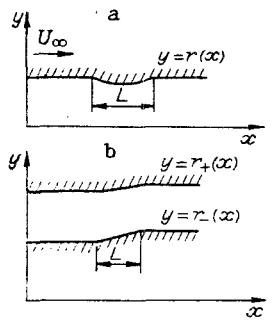

Fig. 1

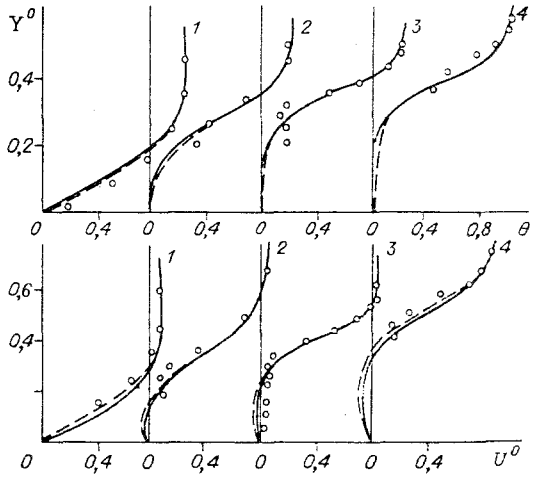

Fig. 2

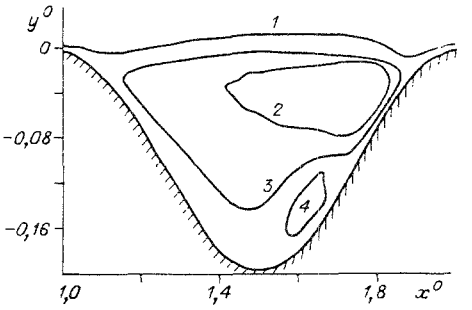

Fig. 3

2. When the above-stated conditions are met, the boundary-layer equations are conveniently written in the variables

$$X = x,\ Y = \pm(y - r_\mp),\ U = u,\ V = \pm(v - u dr_\mp/dx),$$

where u and v are the components of the velocity vector in the coordinates x and y; the upper sign corresponds to the lower wall or free surface, and the lower sign corresponds to the upper wall.

Discarding terms $O(\delta/L) = O(Re^{-1/2})$ and higher in the Navier–Stokes equations [$\Delta_y r = O(\delta)$, so that these terms include terms characterizing the deviation of the direction of the coordinate Y from the normal to the surface], we obtain a system of equations describing the boundary layer with swirl and heat transfer:

$$U\partial U/\partial X + V\partial U/\partial Y = -1/\rho\partial p/\partial X + \Gamma^2/r_\mp^3 dr_\mp/dX + \nu\partial^2 U/\partial Y^2; \quad (2.1)$$

$$(1/\rho)\,\partial p/\partial Y = \pm\Gamma^2/r_\mp^3; \quad (2.2)$$

$$\partial U/\partial X + \partial V/\partial Y = 0; \quad (2.3)$$

$$U\partial\Gamma/\partial X + V\partial\Gamma/\partial Y = \nu\partial^2\Gamma/\partial Y^2; \quad (2.4)$$

$$U\partial T/\partial X + V\partial T/\partial Y = \nu/\mathrm{Pr}\,\partial^2 T/\partial Y^2. \quad (2.5)$$

Here p is the pressure, ρ is the density, T is the temperature, Pr is the Prandtl number, $\Gamma = yw$, and w is the circumferential component of the velocity vector. The energy equation (2.5) is written with allowance for the fact that the investigated flow involves an incompressible fluid with a temperature factor close to unity.

We note that when swirl is absent ($\Gamma \equiv 0$), the equations for the boundary layer on a surface of revolution coincide with the equations for a planar boundary layer in the given approximation [$r_\mp \gtrsim L$, $\Delta_y r_\mp = O(\delta)$]. Swirl can also be disregarded if it is weak or moderate, i.e., if $\Gamma/U_\infty r \lesssim 1$. Indeed, if follows from Eq. (2.2) that $\Delta p = O(Re^{-1/2})$ and, hence, the variation of the pressure across the boundary layer is of the next higher order of smallness in comparison with the other terms in the equations. The term containing Γ on the right-hand side of Eq. (2.1) is also $O(Re^{-1/2})$ and can be ignored. The influence of strong swirl on the flow is appreciable. For example, if $\Gamma/U_\infty r = O(Re^{1/4})$, all the terms in Eq. (2.1) are of the same order. However, an analysis of self-similar solutions (see Sec. 5 below) and the results of calculations by the direct–inverse method in cases where swirl induces flow separation show that a solution exists only for $\Gamma/U_\infty r < \mathrm{const}\, Re^{1/4}$. The system (2.1)-(2.5) can therefore be used to describe swirled flows with a parameter Γ in the range $1 \ll \Gamma/U_\infty r \ll Re^{1/4}$. The effect of variation of the pressure across the boundary layer is not as significant here as the effect associated with curvature of the surface.

Outside the boundary layer, Eqs. (2.1)-(2.5) go over to

$$U_e\partial U_e/\partial X = -(1/\rho)\partial p_e/\partial X + \Gamma_e^2/r_\mp^3 dr_\mp/dX; \quad (2.6)$$

$$(1/\rho)\,\partial p_e/\partial Y = \pm\Gamma_e^2/r_\mp^3 \quad (2.7)$$

(the subscript e refers to the values of the parameters in the limit $Y \to \infty$). Eliminating the pressure in Eq. (2.1) by means of (2.2), (2.6), and (2.7), we arrive at the equation

$$U\partial U/\partial X + V\partial U/\partial Y = \beta + (\Gamma^2 - \Gamma_e^2)/r_\mp^3 dr_\mp/dX \pm \partial\left(\int_Y^\infty (\Gamma^2 - \Gamma_e^2)/r_\mp^3 dY\right)/\partial X + \nu\partial^2 U/\partial Y^2 \qquad (2.8)$$

($\beta = U_e dU_e/dX$). Consequently, the relations (2.3)-(2.5), (2.8) must be integrated in order to calculate the boundary layer.

The boundary conditions have the form

$$U = V = \Gamma = 0,\ T = T_w \text{ for } Y = 0,\ \partial U/\partial Y \to 0,\ \Gamma \to \Gamma_e,$$
$$T \to T_e \text{ for } Y \to \infty, \qquad (2.9)$$

where T_w is the temperature of the surface, and Γ_e and T_e are the circulation and temperature in the external flow on the contour corrected for the displacement thickness, thus ensuring proper matching in these variables.

In the inverse boundary-layer problem the parameter β is not known beforehand, and its determination requires that the distribution of the displacement thickness be specified:

$$\int_0^\infty (1 - U/U_e)\, dY = \delta(X). \qquad (2.10)$$

The distribution of the parameters U(0, Y), Γ(0, Y), T(0, Y) must be specified in the initial cross section $X = X_0$.

The following condition is necessary in order to match the solutions in the boundary layer and in the external flow:

$$U_e(X) = u_e(X) \qquad (2.11)$$

[$u_e(X)$ is the velocity of the external inviscid flow on the contour correct for the displacement thickness, i.e., at $y = r_\mp \pm \delta_\mp$]. The equation of continuity can be used to show that the satisfaction of condition (2.11) also guarantees matching of the transverse components of the velocity vector. Condition (2.11) enables us to determine $\delta(X)$, which can be done iteratively: U_e and u_e are found for a given δ, and if (2.11) is not satisfied, then δ is corrected, etc.

3. The linear approximation is used in the present study to calculate the external flow velocity. For example, in the calculation of flow over a free surface $y = r(x)$ the external planar flow is assumed to be potential, and the theory of slender bodies can be used to obtain an integral representation for u_e [1]:

$$u_e(X) = U_\infty\left(1 + (1/\pi)\int_{-\infty}^{\infty} dr/d\xi/(X - \xi)\, d\xi\right). \qquad (3.1)$$

In the case of channel flow we assume that $w_e = \Gamma_e/r$, i.e., it is swirled according to the free vortex law (Γ_e = const) and, accordingly, is also potential flow. To simplify the problem, we consider the case of a narrow channel, i.e., $(r_+ - r_-)/r_- \ll 1$; the flow in the meridian plane can then be regarded as planar. The results of numerical solution of the equation for the stream function of potential flow by means of the same computer program as that used in [3] shows that the velocities on the contour differ by less than 1% in the planar and axisymmetrical cases for $(r_+ - r_-)/r_- \lesssim 0.1$. We obtain the following equations for the velocity of potential flow in a plane channel with parallel walls along the entrance and exit zones [$dr_\pm/dx = 0$ at $|x| > |x_L|$, where $x_L = O(L)$] and with a slightly perturbed contour along the transition zone [$\Delta_y r_\pm = O(\delta)$, i.e., this quantity is a small parameter], by analogy with [4]:

$$U_{e\mp} = U_\infty\left(R_0 + \int_{-\infty}^{\infty} (K((X - \xi)/R_0)\, dr_\mp/d\xi + K_1((X - \xi)/R_0) dr_\pm/d\xi) d\xi\right)/R(X). \qquad (3.2)$$

Here $R(X) = r_+(X) - r_-(X)$; $R_0 = R(-\infty)$; $K(X) = (1/2)\,\mathrm{sgn}\,(X)(\coth \pi|X|/2 - 1)$, and $K_1(X) = (1/2)\,\mathrm{sgn}\,(X)(1 - \tanh \pi|X|/2)$. Equations (3.2) are valid to within terms $O(|\Delta y r|^2)$.

To calculate the parameters on the contour corrected for the displacement thickness, we need to replace $r_\pm$ by $r_\mp \pm \delta_\mp$ in Eqs. (3.1) and (3.2). In the numerical calculations the integrals are evaluated on a finite interval, outside of which $dr/dX = 0$, and the contribution of $d\delta/dX$ can be disregarded. The length of the interval must be determined from the condition that the result is independent of the limits of integration.

Calculations of separation flows according to the above-described direct–inverse method have been carried out by the numerical algorithm in [3]. Equations (2.3)-(2.5), and (2.8)

are integrated by a finite-difference scheme of second-order precision. The integrals in Eqs. (3.1) and (3.2) are calculated by the trapezoidal rule. An iterative procedure [3] taking into account the nonlocal character of the relationship of δ to U_e and u_e is used to find $\delta(X)$ according to (2.11).

4. To assess the possibilities of calculating separation flows in the presence of heat transfer, we investigate flow over a cavity, whose shape is described by the equation $r(x)/L = -0.1[1 - \cos 2\pi(x^0 - 1)]$ for $1 \leqslant x^0 \leqslant 2$ and $r(x) = 0$ for $x^0 > 2$, < 1, where $x^0 = x/L$. The Reynolds number is $Re = 1.21 \cdot 10^4$, the freestream temperature is $T_e = 71°C$, and the surface temperature is $T_w = 56°C$, i.e., the temperature factor is $T_w/T_e = 0.96$. This flow has been investigated experimentally [6] and calculated in the same work on the basis of the complete system of Navier–Strokes equations.

In calculating the velocity distribution $U^0 = U/U_\infty$ and the excess temperature $\theta = (T - T_w)/(T_e - T_w)$ in the cross section $x^0 = 0$, a Blasius profile with displacement thickness $\delta_0/L = 2.5 \cdot 10^{-2}$ is specified, and the Prandtl number is assumed to be equal to 0.75. A 61 × 60 grid is used to calculate the boundary layer. A solution of the interaction problem is obtained by an iterative procedure after 20 iterations; the printout on the digital printer of a Unified Series ES-1061 computer is approximately 2 min.

Figure 2 shows the velocity and excess temperature profiles obtained in the present study (solid curves) and the results of measurements (points) and calculations (dashed curves) from [6]. Here $Y^0 = 10Y/L$, $x^0 = 1.0$, 1.2, 1.4, and 1.6 (curves 1-4). The results calculated by means of the boundary-layer equations are in good agreement with those obtained on the basis of the Navier–Stokes equations. The correspondence between the calculated and measured velocity profiles is also fully satisfactory. The agreement is not so good between the calculated and experimental temperature profiles in the separation zone; the discrepancies are probably attributable to transient phenomena in the experiment (Saidi et al. [6] mention unsteadiness on the part of the flow), which are ignored in the calculations.

The streamline pattern shown in Fig. 3, where curves 1-4 correspond to stream functions $\psi/U_\infty L = 0.02$, -0.01, -0.002, 0.0005. A primary vortex fills up most of the cavity, and a small secondary vortex is formed on the bottom. The same structure has been obtained [6] by means of the Navier–Stokes equations. Figure 4 shows the pattern of isographs of the excess temperature $\theta = 0.1$, 0.04, 0.01, 0.005 (curves 1-4, respectively), where the location of the reattachment point is indicated by an arrow. Clearly, the isographs bunch up in the vicinity of this point, consistent with the increased heat flux in the region.

On the whole, we can conclude that the boundary-layer equations can be used to describe flows with thin separation zones in the presence of heat transfer within the same error limits as when the Navier–Stokes equations are used.

5. We now consider the self-similar solutions of the system (2.3), (2.4), (2.8) in the presence of swirl. The self-similar solutions of the boundary-layer equations with swirl have been investigated previously [7] for nonseparation flow regimes and for a constant pressure across the layer. The additional term in Eq. (2.8) restricts the class of admissible self-similar solutions, but then these solutions have somewhat different properties anyway. It is also interesting to investigate self-similar solutions corresponding to flow with reverse currents.

We assume below that the external flow is swirled according to the free vortex law, i.e., $\Gamma_e = \text{const}$. In this case the system (2.3), (2.4), (2.8) has self-similar solutions under the condition $r = r_0 = \text{const}$, $U_e = U_0 X^{1/5}$. The solutions form a single-parameter family, whose parameter depends on Γ_e. However, if $r = r_0 + r_1 X^{2/5}$ and $r_1 X^{2/5} \ll r_0$, we can disregard terms containing $r_1 X^{2/5}/r_0$ in Eq. (2.8), whereupon we obtain an auxiliary two-parameter family of self-similar solutions, in which the solutions of the first type are subsumed as a special case.

The self-similar solutions have the form

$$\eta = (3/5U_0/\nu)^{1/2} Y/X^{2/5}, \; U/U_e = f'(\eta),$$
$$V = -((3/5U_0/\nu)^{1/2}/X^{2/5})(f - 2/3\eta f'(\eta)), \; \Gamma/\Gamma_e = g(\eta), \tag{5.1}$$

where the prime signifies differentiation with respect to the variable η. In these variables Eqs. (2.3), (2.4), (2.8) and the boundary conditions (2.9) are transformed as follows:

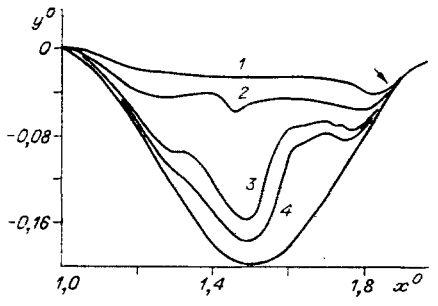

Fig. 4

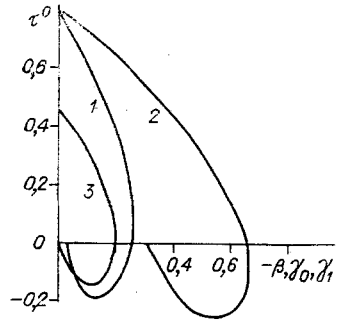

Fig. 5

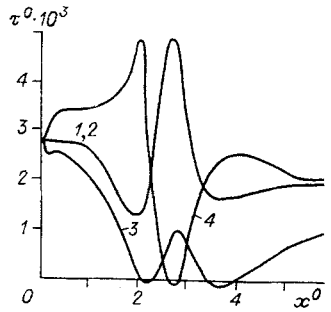

Fig. 6

$$f''' + ff'' + (1/3)(1 - f'^2) + \gamma_0\left(\int_\eta^\infty (g^2 - 1)\,d\eta + (g^2 - 1)\,\eta\right) + \gamma_1(g^2 - 1) = 0; \tag{5.2}$$

$$g'' + fg' = 0; \tag{5.3}$$

$$f(0) = f'(0) = g(0) = 0,\ f'(\infty) \to 1,\ g(\infty) \to 1. \tag{5.4}$$

Here $\gamma_0 = \pm 2\Gamma_e^2/3r_0U_0^2(5\nu/3U_0)^{1/2}$; $\gamma_1 = 2\Gamma_e^2 r_1/3r_0^3U_0^2$; values of $\gamma_0 > 0$ correspond to the boundary layer on the exterior side of a surface of revolution (or the lower wall of a channel), and $\gamma_0 < 0$ corresponds to the boundary layer on the interior side (or the upper wall of a channel). The sign of γ_1 is determined by the slope of the generatrix of the surface of revolution relative to the axis of revolution: $\gamma_1 > 0$ if the generatrix is slanted away from the axis, and $\gamma_1 < 0$ if the generatrix is slanted toward the axis. Without swirl ($\gamma_0 = \gamma_1 = 0$) the self-similar solution corresponds to the Faulkner–Skan self-similar solution with self-similarity parameter $\beta = 1/3$. If $\gamma_0 = 0$ and $\gamma_1 \neq 0$, Eqs. (5.2)-(5.4) coincide with the self-similar equations in [7].

Since $0 \leqslant g \leqslant 1$, the signs of γ_0 and γ_1 determine the sign of the swirl-induced longitudinal pressure gradient. Swirl tends to accelerate the flow in the boundary layer on the interior side of a surface of revolution ($\gamma_0 < 0$) or when the generatrix of the surface slants toward the axis ($\gamma_1 < 0$). In this case the velocity inside the boundary layer can be greater than the external flow velocity. Swirl tends to decelerate the flow in the boundary layer and can induce separation on the exterior side of a surface of revolution ($\gamma_0 > 0$) or when the generatrix of the surface slants away from the axis ($\gamma_1 > 0$), even on a cylindrical surface and in the presence of accelerated external flow. It is evident from these considerations that the onset of a separation zone on the lower wall of an annular cylindrical channel will be inevitable as the swirl intensity increases, whereas the flow on the upper wall will be accelerated.

To determine the range of parameters in which self-similar solutions with reverse currents are possible, we examine two cases: $\gamma_1 = 0$, $\gamma_0 > 0$ and $\gamma_0 = 0$, $\gamma_1 > 0$. The system of equations (5.2)-(5.4) is integrated numerically by a finite-difference procedure similar to the numerical method used to solve the inverse problem for nonself-similar solutions; the analog of the displacement thickness in this case is the quantity $\int_0^\infty (1 - f')\,d\eta$. The quantity $\tau^0 =$ f"(0), which is proportional to the frictional stress on the wall, is shown in Fig. 5 as a function of the parameters γ_0 (curve 1) and γ_1 (curve 2). Also shown in the figure for comparison is the well-known dependence of τ^0 on $(-\beta)$, where β is the self-similarity parameter in the Faulkner–Skan solution (curve 3). Solutions exist for $\gamma_0 \lesssim 0.265$ and $\gamma_1 \lesssim 0.660$. These limiting values are branch points of the solutions; a single value of γ_0 (γ_1) corresponds to solutions with and without reverse currents, i.e., the properties of these solutions are qualitatively the same as those of the Faulkner–Skan solutions.

Inasmuch as $\gamma_0 \sim (\Gamma_e/U_e r_0)^2 L/r_0\,\mathrm{Re}^{1/2}$ and $\gamma_1 \sim (\Gamma_e/U_e r_0)^2(\Delta_y r/r_0)$, the constraints on γ_0 and γ_1 by virtue of the conditions $r_0 = O(L)$ and $\Delta yr = O(\delta)$ yield the following upper bound on the possible swirl intensity:

$$\Gamma_e/U_e r_0 \leqslant \mathrm{const}\,\mathrm{Re}^{1/4}. \tag{5.5}$$

It occurs when swirl induces an unfavorable longitudinal pressure gradient. As mentioned, this situation prevails at the lower wall, so that condition (5.5) determines the maximum attainable swirl intensity in a channel according to the free vortex law in the given approximation.

6. The qualitative results obtained on the influence of swirl from an analysis of the self-similar solutions are corroborated by the solution of the viscous-inviscid interaction problem according to the direct–inverse method. We now discuss flow in a dogleg channel (Fig. 1b), whose wall contours are given by the relations $r_-(x^0)/L = 10$ for $x^0 < 2$, $r_-(x^0)/L = 10 + 0.08(x^0 - 2)[3 - 2(x^0 - 2)]$ for $2 \leqslant x^0 \leqslant 3$, and $r_-(x^0)/L = 10.08$ for $x^0 > 3$; $r_+(x^0)/L = r_-(x^0)/L + 1$. The Reynolds number is equal to $6.25 \cdot 10^3$, the flow core is assumed to be swirled according to the free vortex law, and the swirl intensity is varied over the interval $0 \leqslant \Gamma_e/U_\infty r_- \leqslant 5$. The flow temperature is assumed to be constant, i.e., heat transfer is ignored. In the initial cross section ($x^0 = 0$) the velocity in the flow core is assumed to be constant across the channel, and the distributions of the velocity U and the circulation Γ are specified by a Blasius profile, where the displacement thickness $\delta_-/L = \delta_+/L = 3 \cdot 10^{-2}$. A 150 × 60 differencing grid is used to compute the boundary layers. Approximately 15 iterations are required to obtain a solution of the interaction problem, and the time to compute one set of results (for a given swirl regime) is approximately 5 min on the ES-1061 computer.

Figure 6 shows the results of friction calculations from the longitudinal component of the velocity on the lower wall (curves 1-3) and upper wall (curve 4) of a channel, where $\tau^0 = \nu \partial U/\partial Y|_{X, Y=0}/U_\infty^2$, and $\Gamma_e/U_\infty r_- = 0$, 1, 4, 4 (curves 1-4, respectively). Clearly, unswirled channel flow does not separate, because the cross section of the channel remains essentially constant. The influence of swirl at moderate intensities ($\Gamma_e/U_\infty r_- = 1$) is insignificant, and the results scarcely differ from the preceding case. A further increase in the swirl intensity ($\Gamma_e/U_\infty r_- = 4$) leads to flow separation. Since the angle between the generatrices of the upper and lower walls of the channel and the axis is positive in the transition section (dogleg), swirl induces flow separation on both the lower and the upper wall (curves 3 and 4 in Fig. 6). Following the dogleg, the transverse pressure difference creates a second separation zone on the lower wall (curve 3).

In an attempt to increase the swirl intensity to $\Gamma_e/U_\infty r_- = 5$, we have been unable to obtain a convergent solution of the interaction problem, evidently because the upper bound (5.5) is reached in this case ($\mathrm{Re}^{1/4} \approx 9$ in the given example).

The foregoing results show that the boundary-layer equations can be used to calculate heat transfer in thin closed separation zones and to determine the conditions under which flow separation takes place in the presence of swirl. Calculations can be performed with very small expenditures of computer time in situations where the given approximation is applicable.

LITERATURE CITED

1. J. E. Carter, "Solutions for laminar boundary layers with separation and reattachment," AIAA Paper No. 583, AIAA, New York (1974).
2. H. McDonald and W. R. Briley, "A survey of recent work on interacted boundary-layer theory for flow with separation," in: Numerical and Physical Aspects of Aerodynamic Flows II, Springer-Verlag, Berlin–New York (1984).
3. V. I. Vasil'ev, S. V. Khokhlov, and E. Yu. Shal'man, "Calculation of separation flows by means of boundary-layer equations," Prikl. Mekh. Tekh. Fiz., No. 6 (1990).
4. V. I. Vasil'ev, "Calculation of viscous incompressible fluid flow in a channel with a separator and determination of its global characteristics," Izv. Akad. Nauk SSSR, Mekh. Zhidk. Gaza, No. 1 (1991).
5. T. Cebeci and P. Bradshaw, Physical and Computational Aspects of Convective Heat Transfer, Springer-Verlag, Berlin–New York (1991).
6. C. Saidi, F. Legay-Desesquelles, and B. Prunet-Foch, "Laminar flow past sinusoidal cavity," Int. J. Heat Mass Transfer, 30, No. 4 (1987).
7. V. V. Bogdanova, "Laminar boundary layer in axisymmetrical swirled flow," in: Engineering Fluid and Gas Dynamics (Proceedings of the Leningrad Polytechnic Institute, No. 248) [in Russian], LPI, Leningrad (St. Petersburg) (1965).